



A New Semi Analytical Method for Solving Some Non-Linear Infinite Boundary Value Problems in Physical Sciences

R. R. Subanya, V. Ananthaswamy*  and S. Sivasankari

Research Centre and PG Department of Mathematics, The Madura College (affiliated to Madurai Kamaraj University), Madurai, Tamil Nadu, India

*Corresponding author: ananthu9777@gmail.com

Received: December 8, 2022

Accepted: May 2, 2023

Abstract. One new approximate analytical method called Ananthaswamy-Sivasankari method for third order boundary value problems is applied to acquire the approximate solutions to some physical science problems, particularly Magnetohydrodynamic (MHD) casson fluid flow and MHD boundary layer flow analytically. The numerical and approximate analytical solutions to these equations are then compared and the results demonstrate a very good agreement. The resulting approximate analytical expressions are provided in an explicit and closed form. The outcomes demonstrated that the new approximate analytical method is more practical and simple to understand. Furthermore, a graphic interlining of the obtained findings is provided.

Keywords. Magnetohydrodynamic (MHD) boundary layer flow, Casson fluid, Boundary value problem, Stretching/Shrinking sheet, Ananthaswamy-Sivasankari method (ASM), Homotopy analysis method (HAM)

Mathematics Subject Classification (2020). 34B40, 34E05, 34E10, 34E15, 34E20

Copyright © 2023 R. R. Subanya, V. Ananthaswamy and S. Sivasankari. *This is an open access article distributed under the Creative Commons Attribution License, which permits unrestricted use, distribution, and reproduction in any medium, provided the original work is properly cited.*

1. Introduction

Recent years researchers have shown a tremendous interest to do research in the domain of MHD boundary layer flow due to its wide range of applications in engineering and industries such as drawing of plastic films, extrusion processes in plastic and metal industries. Ariel [3]

examined an approximate solution for the flow with suction at the stagnation point. The analytic solution for MHD boundary layer flows in Casson fluid across a stretching/shrinking sheet involving wall mass transfer was discovered by Battacharyya *et al.* [4]. Bhattacharyya [5] used the finite difference technique to investigate the effects of heat source and sink on such a steady two-dimensional MHD boundary layer motion and thermal radiation over a sheet that is shrinking and has wall mass suction. Crane [6] developed a closed form solution for steady two-dimensional stretching in which the velocity on the boundary is away from the fixed point and proportional to the distance.

Fang and Zhang [7] obtained the closed and exact analytical expression of the governing Navier-Stokes equations for the MHD flow across a periodically shrinking surface. The unstable viscous fluid flow along a continuously moving shrinking surface having mass suction was studied in Fang *et al.* [9]. The heat transfer parameters from the shrinking sheet problem with a linear velocity were described by Fang and Zhang [8]. The MHD flow of a second-grade fluid through a shrinking sheet was taken into consideration by Hayat *et al.* [10] who also came out with the analytical solution for the problem using HAM and series solution. Ibrahim and Makinde [11] presented a boundary layer analysis for Casson nanofluid flow over a stretching sheet with slip and convective boundary under MHD stagnation point flow.

The analysis of MHD boundary layer flow past a stretching plate with heat transfer has been explored by Jhankal and Kumar [12]. Using a shooting technique and a Runge-Kutta-Fehlberg integration strategy, Khan *et al.* [14] evaluated the non-aligned hydro magnetic stagnation point flow of a water base variable viscosity nanofluid across a convectively heated stretching sheet with radiative heat numerically. For the purpose of resolving a non-linear third order boundary value problem across an infinite domain, Kravnchenko and Yablonskii [15, 16] used the Dirichlet series. In a stretching surface, the set of equations for boundary layer was addressed in Kudenatti *et al.* [17]. Magyari and Keller [19] evaluated and compared the heat and mass-transfer properties of the boundary layers upon an exponentially stretching constant surface to the well-known results of power-law models.

A numerical study of the free convection flow in a nanofluid caused by the motion of a constantly stretching sheet has been carried out by Makinde and Aziz [21]. Sakiadis [31] conducted ground-breaking research in this field by examining the free convection fluid flow on such a continually stretching surface at constant speed. The work of Sakiadis was empirically validated in Tsou *et al.* [32]. After reviewing the work of Sakiadis, other researchers [20, 23] generalized the surface boundary conditions. Makinde [22] have described the effects of convective cooling on nanofluid flow over an unsteady stretching sheet. The viscous flow caused only by a shrinking sheet was researched by Micklavčič and Wang [25].

With the aid of HAM, Liao [18] found a brand-new branch of solutions for boundary-layer flows over a stretched impermeable wall. In order to determine how a casson fluid would flow in the region of a stagnation point toward a stretching sheet, Mustafa *et al.* [26] computed the analytical solution. Nadeem *et al.* [28] have explored the MHD flow for a casson fluid across

an exponentially shrinking sheet using ADM. The thin film flow on a fluctuating shrinking sheet through it with a porous media with dynamic viscosity was highlighted by Nadeem and Awais [27]. Under a thin liquid layer of a modulating stretching sheet, Noor *et al.* [29] used Homotopy analysis method to study heat transfer and MHD flow. Noor *et al.* [30] used a straightforward non-perturbative approach to deal with MHD viscous flow caused there by a shrinking sheet. Wang [34] addressed the problem that Stagnation flow onto a shrinking sheet. The exact solutions to the steady free state Navier-Stokes equations were established by Wang [33].

The primary goal of this present paper is to introduce a different approximate analytical method known as Ananthaswamy-Sivasankari Method for third order boundary value problems. By applying this approach to a few third order non-linear boundary value problems that exist in physical science, like MHD casson fluid flow and MHD boundary layer flow. The analytical results are compared with the numerical results. Additionally, the data are plotted to highlight how different physical characteristics affect the outcome.

2. Ananthaswamy-Sivasankari Method (ASM)

For the purpose of evaluating the third order non-linear ordinary differential equations, a new method called Ananthaswamy-Sivasankari method (ASM) is introduced. One can use it to resolve both linear as well as non-linear differential equations. This method can also be easily extended to resolve some other non-linear such boundary value problems in physical, chemical and biological sciences, especially for MHD boundary layer flow problems in physical science. However the proposed new method is applicable to boundary value issues. For the differential equation and its derivatives, additional boundary conditions can be generated.

2.1 Basic Concept of ASM

Let us consider the non-linear boundary value problem

$$q : f(y, y', y'', y''') = 0, \tag{2.1}$$

where q represents the third order non-linear differential equation such that $y = y(x, c, d, \dots)$ in which c, d are given parameters and $x \in [L, U]$ can be finite with the following boundary conditions

$$\left. \begin{aligned} \text{At } x = L, \quad & y(x) = y_{L_0} \quad (\text{or}) \quad y'(x) = y_{L_1} \quad (\text{or}) \quad y''(x) = y_{L_2} \\ \text{At } x = U, \quad & y(x) = y_{U_0} \quad (\text{or}) \quad y'(x) = y_{U_1} \quad (\text{or}) \quad y''(x) = y_{U_2} \end{aligned} \right\} \tag{2.2}$$

Assume that the approximate analytical solution of the non-linear equations is an exponential function of the form

$$y(x) = l + me^{ax} + ne^{-ax}. \tag{2.3}$$

The unknown coefficients l, m and n are obtained by solving the non-linear differential equations as follows:

$$\left. \begin{aligned} y(L) &= l + me^{aL} + ne^{-aL} = y_{L_0} \\ y'(L) &= ame^{aL} - ane^{-aL} = y_{L_1} \\ y''(L) &= a^2me^{aL} + a^2ne^{-aL} = y_{L_2} \end{aligned} \right\} \tag{2.4}$$

$$\left. \begin{aligned} y(U) &= l + me^{aU} + ne^{-aU} = y_{U_0} \\ y'(U) &= ame^{aU} - ane^{-aU} = y_{U_1} \\ y''(U) &= a^2me^{aU} + a^2ne^{-aU} = y_{U_2} \end{aligned} \right\} \tag{2.5}$$

Equations (2.4) and (2.5) may be used to get the unknown parameters l, m and n .

The following non-linear differential equations are obtained by substituting an equation (2.3) into the equation (2.1).

$$q : f(y(x, l, m, n, a, c, d), y'(x, l, m, n, a, c, d), y''(x, l, m, n, a, c, d), y'''(x, l, m, n, a, c, d)) = 0. \tag{2.6}$$

This equation is valid at x where $x \in [L, U]$. Solving the equation (2.6), the unknown parameter a can be obtained in terms of given parameters c and d .

3. Examples

In this portion, some examples are solved analytically using ASM and the results are derived very clearly to explain the new method more effective. Examples 3.1 and 3.2 are based on the MHD fluid flow which occurs in physical science.

3.1 Example

Consider the dimensionless form of MHD casson fluid flow over a permeable stretching/shrinking Sheet described in [4, 7, 24] and is given by:

$$\left(1 + \frac{1}{\beta}\right) f''' + f f'' - f'^2 - M^2 f' = 0. \tag{3.1}$$

The dimensionless boundary conditions are given as follows:

For shrinking case

$$f(0) = f_w, \quad f'(0) = -1, \quad f'(\infty) = 0. \tag{3.2}$$

For stretching case

$$f(0) = f_w, \quad f'(0) = 1, \quad f'(\infty) = 0. \tag{3.3}$$

Skin friction co-efficient: The dimensionless local skin friction coefficient is given by

$$Re_x^{1/2} C_f = \left(1 + \frac{1}{\beta}\right) f''(0) \tag{3.4}$$

where Re is the local Reynolds number.

3.1.1 Approximate Analytical Solution using ASM

Case 1: For shrinking sheet

The following is an approximate analytical solution to equation (3.1) that satisfies the boundary

condition as follows:

$$f(\eta) = l + me^{a\eta} + ne^{-a\eta}, \tag{3.5}$$

$$f'(\eta) = me^{a\eta} - ne^{-a\eta}. \tag{3.6}$$

Utilizing the boundary conditions in equation (3.2), we obtain the value of the parameters l, m and n as follows:

$$l = f_w - \frac{1}{a}, \quad m = 0 \quad \text{and} \quad n = \frac{1}{a}. \tag{3.7}$$

Thus, the equation (3.5), becomes

$$f(\eta) = f_w - \frac{1}{a} + \frac{1}{a}e^{-a\eta} \tag{3.8}$$

Now by using the equation (3.8) into an equation (3.1) and on simplification, we get

$$-\left(1 + \frac{1}{\beta}\right)a^2e^{-a\eta} + \left(f_w - \frac{1}{a} + \frac{1}{a}e^{-a\eta}\right)(-ae^{-a\eta}) - e^{-2a\eta} - M^2(-e^{-a\eta}) = 0. \tag{3.9}$$

Now taking $\eta = 0$, equation (3.9) becomes

$$-\left(1 + \frac{1}{\beta}\right)a^2 - f_w a - 1 + M^2 = 0. \tag{3.10}$$

On solving the equation (3.10), we get the value of the parameter a and is given by

$$a = \frac{-f_w\beta \pm \sqrt{f_w^2\beta^2 + 4(M^2\beta^2 + \beta^2 + M^2\beta + \beta)}}{2(\beta + 1)}. \tag{3.11}$$

Hence an approximate analytical solution of the momentum equation (3.1) is obtained by substituting an equation (3.11) into an equation (3.8) as follows:

$$f(\eta) = f_w - \frac{1}{a} + \frac{1}{a}e^{-a\eta} \tag{3.12}$$

where a is obtained in the equation (3.11).

Case 2: For stretching sheet

The following is an approximate analytical solution to equation (3.1) that satisfies the boundary condition as follows:

$$f(\eta) = l + me^{a\eta} + ne^{-a\eta}, \tag{3.13}$$

$$f'(\eta) = me^{a\eta} - ne^{-a\eta}. \tag{3.14}$$

Utilizing the boundary conditions in an equation (3.3), we obtain the value of the parameters l, m and n as follows:

$$l = f_w + \frac{1}{a}, \quad m = 0 \quad \text{and} \quad n = \frac{-1}{a}. \tag{3.15}$$

Thus, the equation (3.13), becomes

$$f(\eta) = f_w + \frac{1}{a} - \frac{1}{a}e^{-a\eta}. \tag{3.16}$$

Now by using the equation (3.16) into an equation (3.1) and on simplification, we get

$$\left(1 + \frac{1}{\beta}\right)a^2e^{-a\eta} + \left(f_w + \frac{1}{a} - \frac{1}{a}e^{-a\eta}\right)(ae^{-a\eta}) - e^{-2a\eta} - M^2(e^{-a\eta}) = 0. \tag{3.17}$$

Now taking $\eta = 0$, equation (3.17) becomes

$$\left(1 + \frac{1}{\beta}\right) \alpha^2 + f_w \alpha - 1 - M^2 = 0. \tag{3.18}$$

On solving the equation (3.18), we get the value of the parameter α and is given by

$$\alpha = \frac{-f_w \beta \pm \sqrt{f_w^2 \beta^2 + 4(M^2 \beta^2 - \beta^2 + M^2 \beta - \beta)}}{2(\beta + 1)}. \tag{3.19}$$

Hence an approximate analytical solution of the momentum equation (3.1) is obtained by substituting an equation (3.19) into an equation (3.16) as follows:

$$f(\eta) = f_w + \frac{1}{\alpha} - \frac{1}{\alpha} e^{-\alpha \eta}. \tag{3.20}$$

where α is obtained in the equation (3.19).

3.2 Example

Consider the problem of MHD boundary layer flow and heat transfer past a shrinking with wall mass suction. With the use of similarity transformation, the following is the transformed non-linear ordinary differential equations presented in [13]:

$$f''' + f f'' - f'^2 - M f' = 0, \tag{3.21}$$

$$\theta'' + Pr(f \theta' - \lambda \theta) = 0. \tag{3.22}$$

The transformed boundary conditions are given by:

$$\left. \begin{aligned} f(0) = S, \quad f'(0) = -1, \quad \theta(0) = 1 \quad \text{at } \eta = 0 \\ \text{and } f'(\eta) \rightarrow 0, \quad \theta(\eta) \rightarrow 0 \quad \text{as } \eta \rightarrow \infty \end{aligned} \right\} \tag{3.23}$$

Skin friction coefficient and Nusselt number

The dimensionless skin friction coefficient is given by:

$$C_f = Re^{-\frac{1}{2}} f''(0). \tag{3.24}$$

The dimensionless Nusselt number is given by

$$Nu = -Re^{\frac{1}{2}} \theta'(0). \tag{3.25}$$

where Re is the local Reynolds number.

3.2.1 Approximate Analytical Solution of Momentum Equation Using ASM

The following is an approximate analytical solution to equation (3.21) that satisfies the boundary condition as follows:

$$f(\eta) = l + m e^{\alpha \eta} + n e^{-\alpha \eta}, \tag{3.26}$$

$$f'(\eta) = m \alpha e^{\alpha \eta} - n \alpha e^{-\alpha \eta} \tag{3.27}$$

Utilizing the boundary conditions in equation (3.23), we obtain the value of the parameters l, m and n as follows:

$$l = S - \frac{1}{\alpha}, \quad m = 0 \quad \text{and} \quad n = \frac{1}{\alpha}. \tag{3.28}$$

Thus, the equation (3.26), becomes

$$f(\eta) = S - \frac{1}{a} + \frac{1}{a}e^{-a\eta}. \tag{3.29}$$

Now by using the equation (3.29) into an equation (3.21) and on simplification, we get

$$-a^2 e^{-a\eta} + \left(S - \frac{1}{a} + \frac{1}{a}e^{-a\eta}\right)(ae^{-a\eta}) - e^{-2a\eta} + M(e^{-a\eta}) = 0. \tag{3.30}$$

Now taking $\eta = 0$, equation (3.30) becomes

$$-a^2 + Sa - 1 + M = 0. \tag{3.31}$$

On solving the equation (3.31), we get the value of the parameter a and is given by

$$a = \pm \frac{S + \sqrt{S^2 - 4 - 4M}}{2}. \tag{3.32}$$

Hence an approximate analytical solution of the momentum equation (3.21) is obtained by substituting an equation (3.32) into an equation (3.29) as follows:

$$f(\eta) = S - \frac{1}{a} + \frac{1}{a}e^{-z\eta}, \tag{3.33}$$

where a is obtained in the equation (3.32).

3.2.2 Approximate Analytical Solution of Energy Equation using HAM ([1,2])

After substituting the equation (3.33) into an equation (3.22), we get the transformed energy equation is as follows:

$$\theta'' + Pr \left(S - \frac{1}{a} + \frac{1}{a}e^{-a\eta}\right)\theta' - Pr \lambda \theta = 0. \tag{3.34}$$

The Homotopy for the equation (3.34) is given by

$$(1 - p)[\theta'' - Pr \lambda \theta] = hp \left[\theta'' + Pr \left(S - \frac{1}{a}\right)\theta' - Pr \lambda \theta + \frac{Pr}{a}e^{-a\eta}\theta'\right]. \tag{3.35}$$

The approximate analytical solution of the equation (3.34) is as follows:

$$\theta = \theta_0 + p\theta_1 + p^2\theta_2 + \dots \tag{3.36}$$

The initial approximations for equation (3.35) is given by

$$\left. \begin{aligned} \theta_0(0) = 1 \text{ and } \theta_i(0) = 0, \quad i = 1, 2, 3, \dots \\ \theta_0(\infty) \rightarrow 0 \text{ and } \theta_i(\infty) \rightarrow 0, \quad i = 1, 2, 3, \dots \end{aligned} \right\} \tag{3.37}$$

Substituting the equation (3.36) into an equation (3.35) and comparing the coefficients of the powers of p , we get the following equations:

$$p^0 : \theta_0'' - Pr \lambda \theta_0 = 0, \tag{3.38}$$

$$p^1 : \theta_1'' - Pr \lambda \theta_1 - [\theta_0'' - Pr \lambda \theta_0] = h \left[\theta_0'' + Pr \left(S - \frac{1}{a}\right)\theta_0' - Pr \lambda \theta_0 + \frac{Pr}{a}e^{-a\eta}\theta_0'\right]. \tag{3.39}$$

Solving the eqns. (3.38) and (3.39), and using the initial approximations equation (3.37), we get the following results.

$$\theta_0 = e^{-B\eta}, \tag{3.40}$$

$$\theta_1 = De^{-B\eta} + Cxe^{-B\eta} + De^{-(a+B)\eta}, \tag{3.41}$$

where

$$B = \sqrt{Pr \lambda}, \quad (3.42)$$

$$C = \frac{-1}{2} h Pr \left(S - \frac{1}{a} \right), \quad (3.43)$$

$$D = \frac{-BhPr}{a[(a+B)^2 - Pr\lambda]}. \quad (3.44)$$

According to HAM technique, we have

$$\theta = \lim_{p \rightarrow 1} \theta(\eta) = \theta_0 + \theta_1. \quad (3.45)$$

Hence an approximate analytical solution of the energy equation (3.22) is obtained by substituting the eqns. (3.40) and (3.41) into an equation (3.45), as follows:

$$\theta(\eta) = e^{-B\eta} + D e^{-B\eta} + C x e^{-B\eta} + D e^{-(a+B)\eta}, \quad (3.46)$$

where B, C and D are obtained in eqns. (3.42), (3.43) and (3.44).

4. Results and Discussion

In this section, we have discussed about the graphical representation for various dimensionless parameters involved in the obtained analytical results in Examples 3.1 and 3.2.

For Example 3.1. Figures 1, 2, 3 represents the comparison between the analytical solution using eqns. (3.12) and (3.20) with the numerical solution presented in [20] for the velocity $f'(\eta)$. Figures 4 and 5 indicates the skin friction coefficient versus the dimensionless parameter f_w .

Figure 1 illustrates that the velocity profile $f'(\eta)$ with the dimensionless axial coordinate η of numerous values of magnetic parameter M and some fixed values of β and f_w . For both shrinking and stretching sheet, by increasing the value of M the velocity decreases. Figure 2 demonstrates that the velocity profile $f'(\eta)$ with the dimensionless axial coordinate η of various values of suction/injection parameter f_w and some fixed values of β and M . For both Shrinking and Stretching sheet, by increasing the value of f_w the velocity decreases. Figure 3 shows that the velocity profile $f'(\eta)$ with the dimensionless axial coordinate η of various values of casson parameter β and some fixed values of f_w and M . For both shrinking and stretching sheet, by increasing the value of β the velocity decreased. Figure 4 depicts the local skin friction coefficient using equation (3.4) with the dimensionless parameter f_w in Stretching sheet for distinct values of magnetic parameter M and casson parameter β . From Figure 4, it is clear that the dimensionless skin friction coefficient increases by increasing M and falls by rising β . Figure 5 interlines the local skin friction coefficient utilizing equation (3.4) with the dimensionless parameter f_w in Shrinking sheet for several values of magnetic parameter and casson parameter β . From Figure 4, it is evident that the skin friction coefficient rises by increasing M and decreases by rising β .

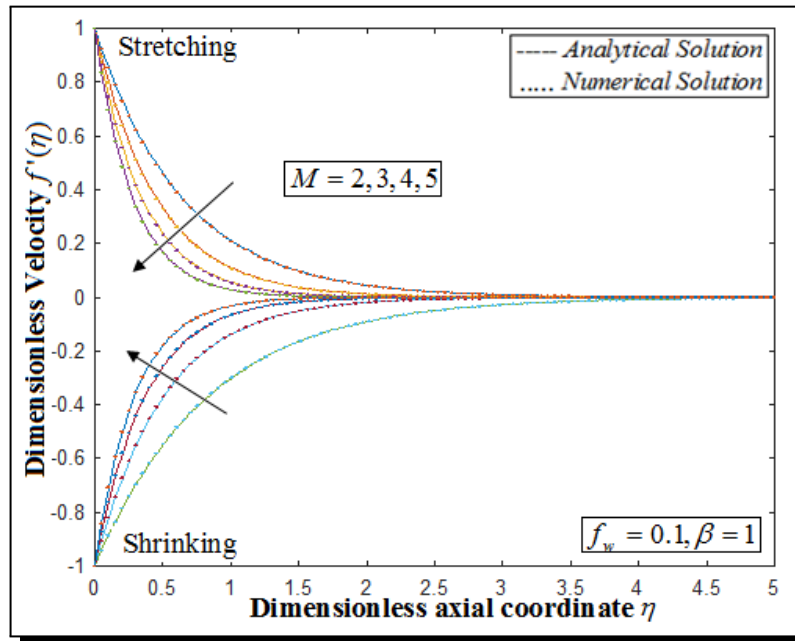


Figure 1. Dimensionless velocity profile $f'(\eta)$ with the dimensionless axial coordinate η of various values of M and some fixed values of β and f_w

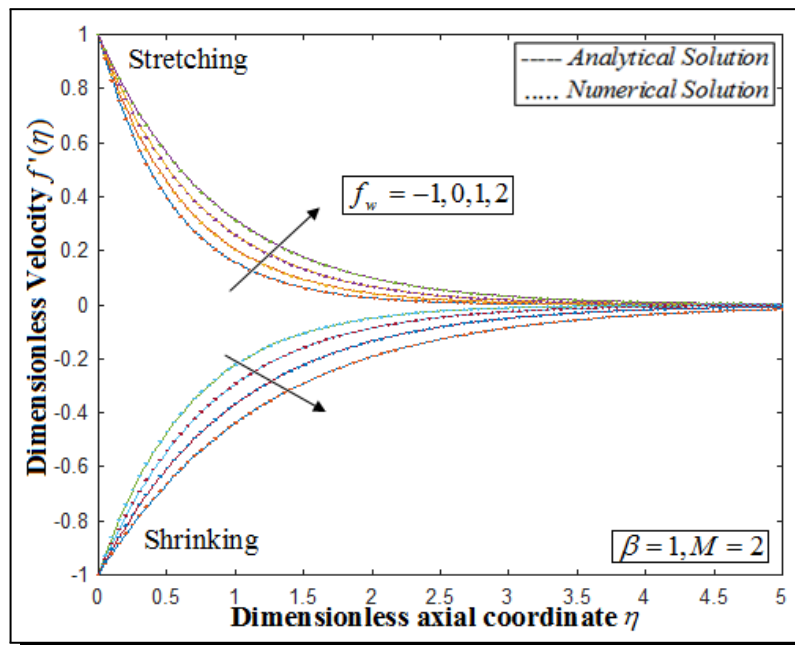


Figure 2. Dimensionless velocity profile $f'(\eta)$ with the dimensionless axial coordinate η of various values of f_w and some fixed values of β and M

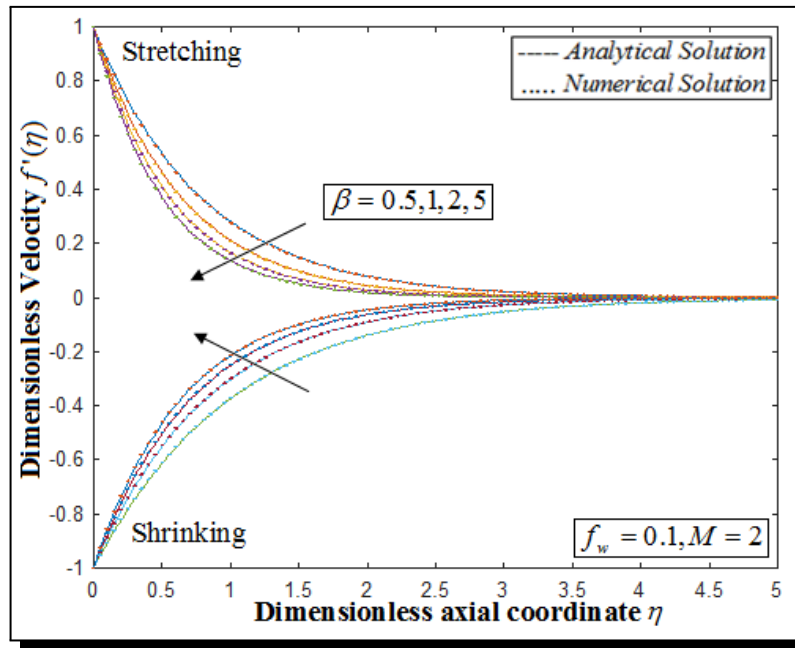


Figure 3. Dimensionless velocity profile $f'(\eta)$ with the dimensionless axial coordinate η of different values of β and certain fixed values of f_w and M

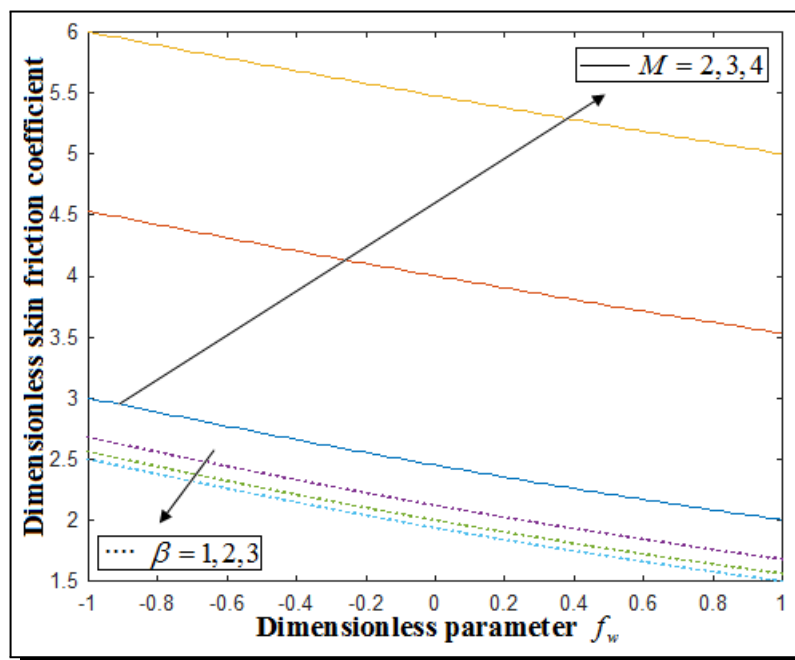


Figure 4. Dimensionless local skin friction coefficient with the dimensionless parameter f_w in Stretching sheet for distinct values of M and β

For Example 3.2. Figures 6 and 7 shows the comparison between the analytical solution using equation (3.33) with the numerical result reported in [13] for the velocity $f'(\eta)$. Figures 8, 9

and 10 displays the comparison between the analytical solution using equation (3.46) with the numerical result reported in [13] for the temperature $\theta(\eta)$. Figure 11 depicts the skin friction $f''(0)$ versus the dimensionless magnetic parameter M . Figure 12 displays the Nusselt Number $\theta'(0)$ versus the dimensionless parameter λ .

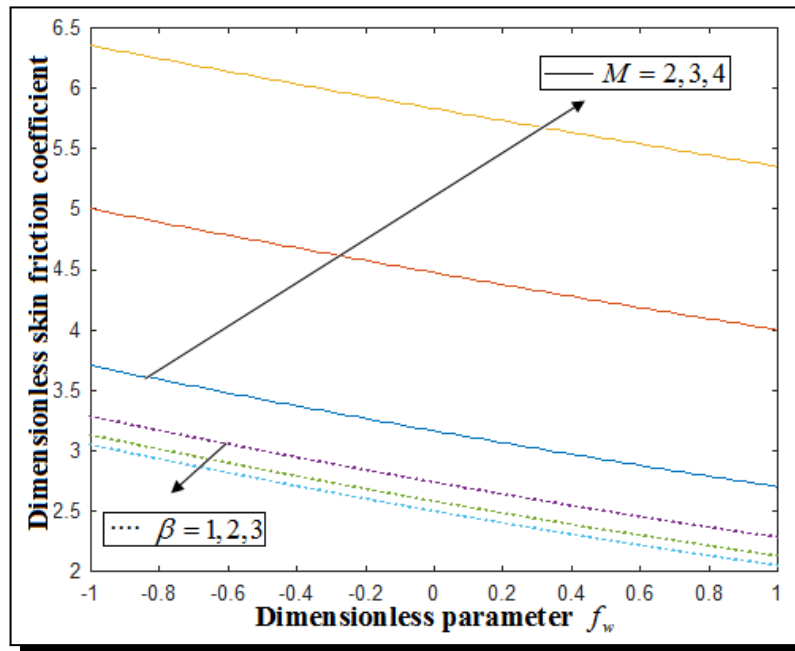


Figure 5. Dimensionless local skin friction coefficient with the dimensionless parameter f_w in Shrinking sheet for several values of M and β

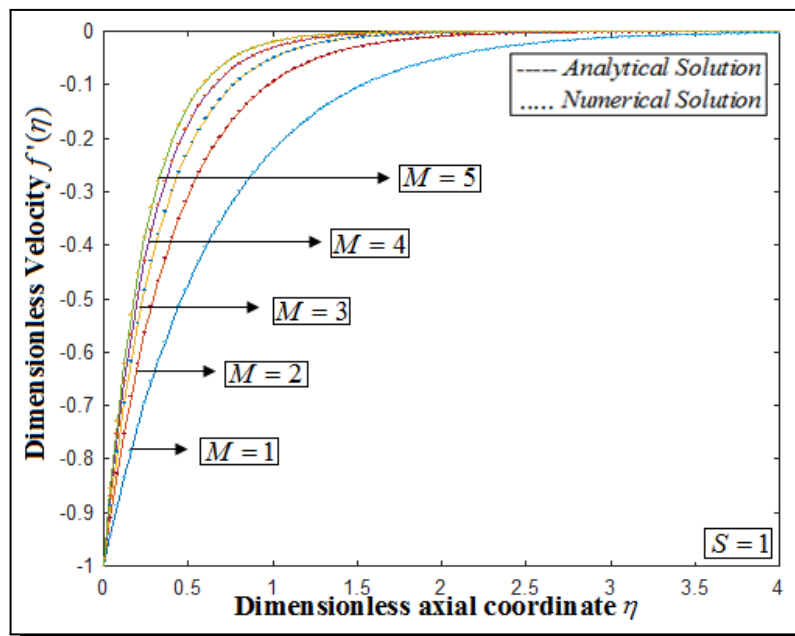


Figure 6. Dimensionless velocity $f'(\eta)$ with the dimensionless axial coordinate η for different values of M and in some fixed amounts of S

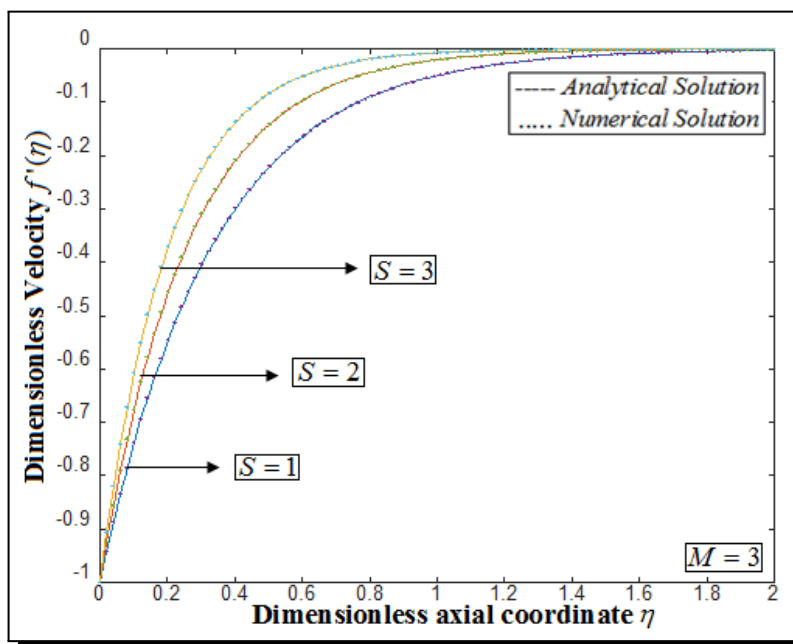


Figure 7. Dimensionless velocity $f'(\eta)$ with the dimensionless axial coordinate η for multiple values of S and in some fixed amounts of M

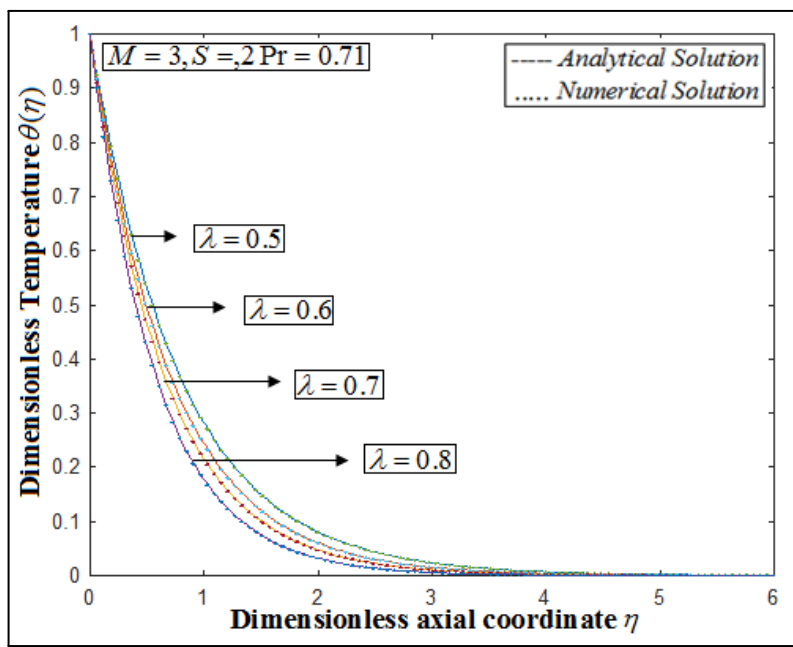


Figure 8. Dimensionless temperature $\theta(\eta)$ with the dimensionless axial coordinate η for varying values of λ and in some specified amounts of S, Pr and M

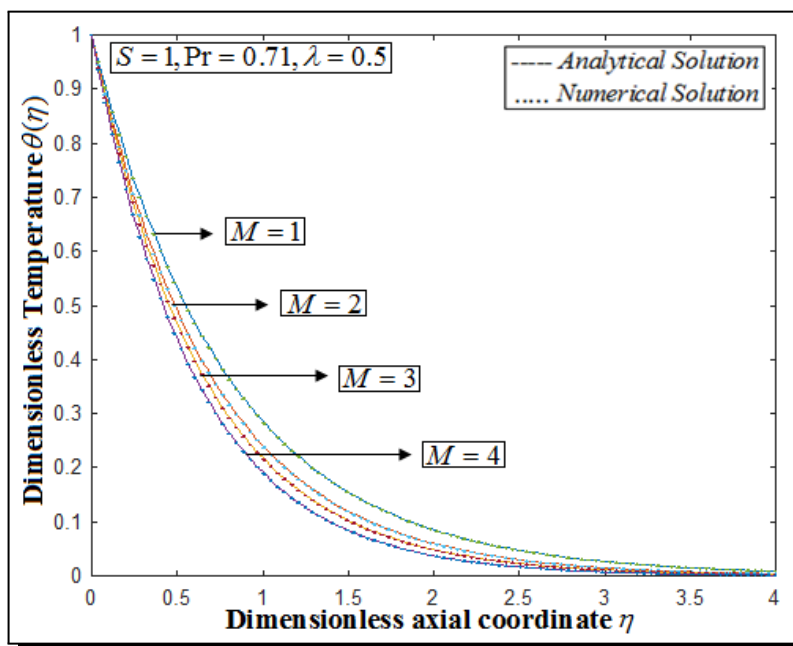


Figure 9. Dimensionless temperature $\theta(\eta)$ with the dimensionless axial coordinate η for various amounts of M and in some particular amounts of S , Pr and λ

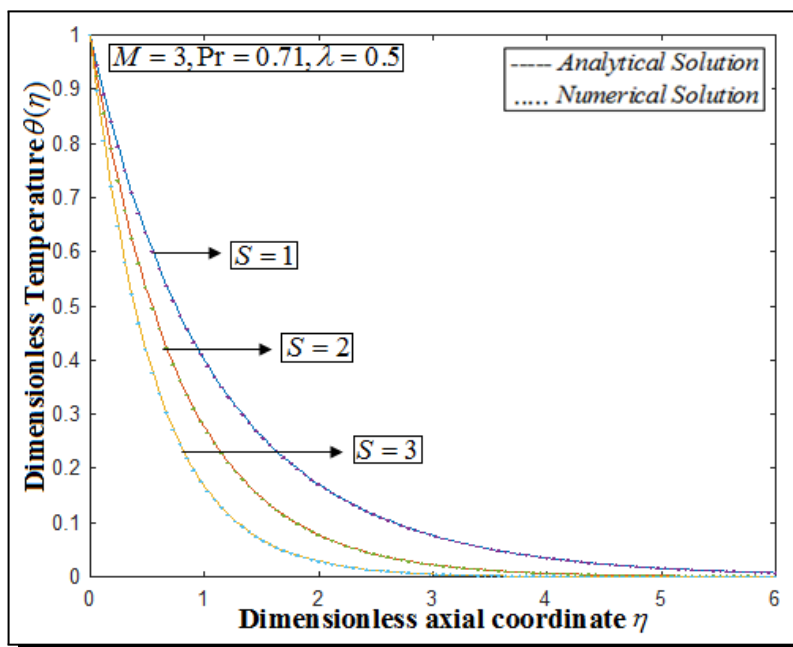


Figure 10. Dimensionless temperature $\theta(\eta)$ with the dimensionless axial coordinate η for distinct values of S and in certain specific amounts of M , Pr and λ

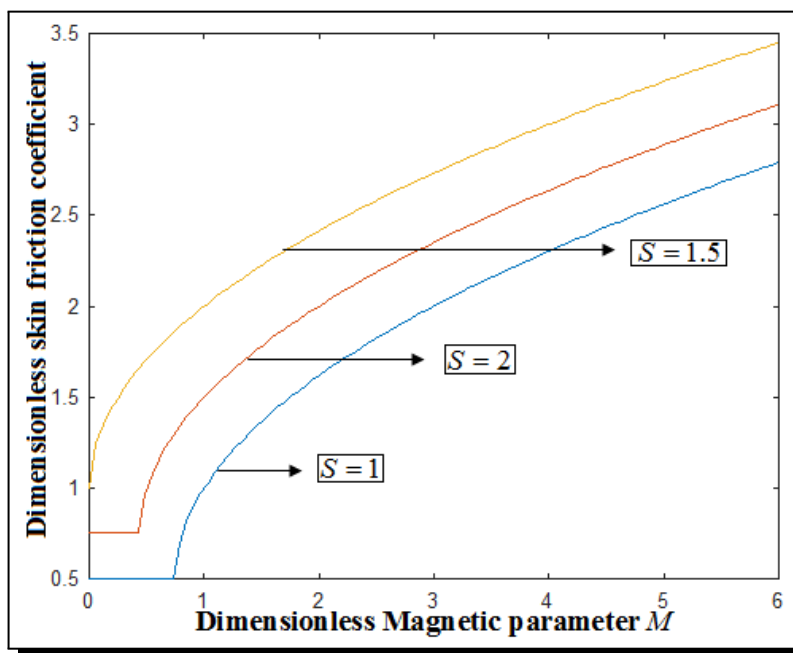


Figure 11. Dimensionless skin friction $f''(0)$ with the dimensionless magnetic parameter M for various values of S

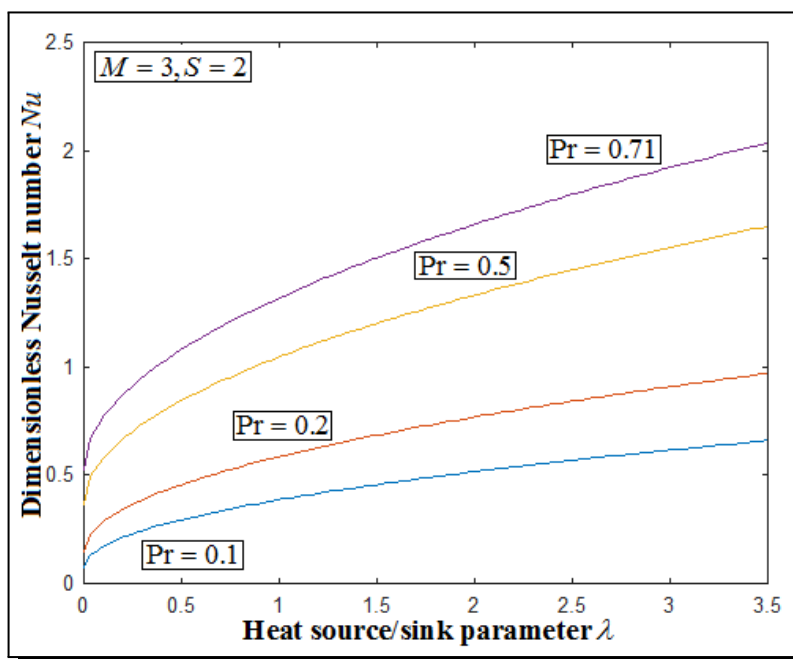


Figure 12. Dimensionless Nusselt Number $\theta'(0)$ with the dimensionless heat source/sink parameter λ for several values of Pr and in some particular values of M and S

Table 1. Comparison of the dimensionless skin friction coefficient using equation (3.4) and the numerical result presented in [5, 24] for numerous values of f_w

	Analytical solution	Numerical solution	Error %
2	2.4142136	2.414214	0.000017
3	3.3027756	3.302776	0.000013
4	4.2360679	4.236068	0.000002
Average error percentage			0.000011

Figure 6 represents the velocity $f'(\eta)$ with the dimensionless axial coordinate η for different values of the magnetic parameter M and in some fixed amounts of S . From this figure, the velocity raises when the value of M is increased. Figure 7 represents the velocity $f'(\eta)$ with the dimensionless axial coordinate η for different values of the suction parameter S and in some fixed amounts of M and by raising the value of S , the velocity increases. Figure 8 shows the temperature $\theta(\eta)$ with the dimensionless axial coordinate η for different values of the heat source/sink parameter λ and in some fixed amounts of S , Pr and M . It can be seen from this figure that, by raising the value of λ , the velocity decreases. Figure 9 interlines the temperature $\theta(\eta)$ with the dimensionless axial coordinate η for different values of M and in some fixed amounts of S , Pr and λ and the velocity decreased by raising the value of the dimensionless parameter M . Figure 10 indicates the temperature $\theta(\eta)$ with the dimensionless axial coordinate η for different values of S and in some fixed amounts of M , Pr and λ . As per this graph, the velocity decreases as the value of the dimensionless parameter S raises. Figure 11 depicts the dimensionless skin friction C_f using equation (3.24) with the dimensionless magnetic parameter M for various values of S . From this figure, it is clear that by raising the parameter S the dimensionless skin friction increases. Figure 12 displays the Nusselt number Nu using equation (3.25) with the dimensionless parameter λ for several amounts of the Prandtl number Pr and in some fixed values of M and S . According to this figure, it is obvious that by raising the parameter Pr the Nusselt number increases.

5. Conclusion

In this current work, the approximate solutions to some physical science problems such as MHD Casson fluid flow and MHD boundary layer flow were found by one new approximate analytical technique called Ananthaswamy-Sivasankari method for third order boundary value problems analytically. The precision of the analytical solution was compared to the numerical solution to these equations, and there was a significant agreement. The explicit and closed form of the approximate analytical result was stated. According to the findings, the new method is more effective and simpler to implement. Also, the results obtained are plotted graphically. This method can be easily extended to solve higher order non-linear boundary value problems.

Appendix A: Basic Concept of the Homotopy Analysis Method ([1, 2])

Consider the following differential equation:

$$N[u(t)] = 0, \tag{A.1}$$

where N is a nonlinear operator, t denotes an independent variable, $u(t)$ is an unknown function. For simplicity, we ignore all boundary or initial conditions, which can be treated in the similar way. By means of generalizing the conventional Homotopy method, Liao constructed the so-called zero-order deformation equation as:

$$(1 - p)L[\varphi(t;p) - u_0(t)] = phH(t)N[\varphi(t;p)], \tag{A.2}$$

where $p \in [0, 1]$ is the embedding parameter, $h \neq 0$ is a nonzero auxiliary parameter, $H(t) \neq 0$ is an auxiliary function, L an auxiliary linear operator, $u_0(t)$ is an initial guess of $u(t)$, $\varphi(t;p)$ is an unknown function. It is important to note that one has great freedom to choose auxiliary unknowns in HAM. Obviously, when $p = 0$ and $p = 1$, it holds:

$$\varphi(t;0) = u_0(t) \text{ and } \varphi(t;1) = u(t), \tag{A.3}$$

respectively. Thus, as p increases from 0 to 1, the solution $\varphi(t;p)$ varies from the initial guess $u_0(t)$ to the solution $u(t)$. Expanding $\varphi(t;p)$ in Taylor series with respect to p , we have:

$$\varphi(t;0) = u_0(t) + \sum_{m=1}^{+\infty} u_m(t)p^m, \tag{A.4}$$

where

$$u_m(t) = \frac{1}{m!} \frac{\partial^m \varphi(t;p)}{\partial p^m} \Big|_{p=0} \tag{A.5}$$

If the auxiliary linear operator, the initial guess, the auxiliary parameter h , and the auxiliary function are so properly chosen, the series (A.4) converges at $p = 1$ then we have:

$$u(t) = u_0(t) + \sum_{m=1}^{+\infty} u_m(t). \tag{A.6}$$

Differentiating (A.2) for m times with respect to the embedding parameter p , and then setting $p = 0$ and finally dividing them by $m!$, we will have the so-called m th-order deformation equation as:

$$L[u_m - \chi_m u_{m-1}] = hH(t)\mathfrak{R}_m(\vec{u}_{m-1}), \tag{A.7}$$

where

$$\mathfrak{R}_m(\vec{u}_{m-1}) = \frac{1}{(m-1)!} \frac{\partial^{m-1} N[\varphi(t;p)]}{\partial p^{m-1}} \tag{A.8}$$

and

$$\chi_m = \begin{cases} 0, & m \leq 1, \\ 1, & m > 1. \end{cases} \tag{A.9}$$

Applying L^{-1} on both side of equation (A.7), we get

$$u_m(t) = \chi_m u_{m-1}(t) + hL^{-1}[H(t)\mathfrak{R}_m(\vec{u}_{m-1})]. \tag{A.10}$$

In this way, it is easily to obtain u_m for $m \geq 1$, at m th order, we have

$$u(t) = \sum_{m=0}^M u_m(t). \quad (\text{A.11})$$

When $M \rightarrow +\infty$, we get an accurate approximation of the original equation (A.1). For the convergence of the above method we refer the reader to Liao [18]. If equation (A.1) admits unique solution, then this method will produce the unique solution.

Competing Interests

The authors declare that they have no competing interests.

Authors' Contributions

All the authors contributed significantly in writing this article. The authors read and approved the final manuscript.

References

- [1] V. Ananthaswamy, C. Sumathi and M. Subha, V. Ananthaswamy, C. Sumathi and M. Subha, Mathematical analysis of variable viscosity fluid flow through a channel and homotopy analysis method, *International Journal of Modern Mathematical Sciences* **14**(3) (2016), 296 – 316.
- [2] V. Ananthaswamy, M. Subha and A. M. Fathima, Approximate analytical expressions of non-linear boundary value problem for a boundary layer flow using the homotopy analysis method, *Madridge Journal of Bioinformatics and Systems Biology* **1**(2) (2019), 34 – 39, DOI: 10.18689/mjbsb-1000107.
- [3] P. D. Ariel, Stagnation point flow with suction: an approximate solution, *Journal of Applied Mechanics* **61**(4) (1994), 976 – 978, DOI: 10.1115/1.2901589.
- [4] K. Battacharyya, T. Hayat and A. Alsaedi, Analytic solution for magnetohydrodynamic boundary layer flow of Casson fluid over a stretching/shrinking sheet with wall mass transfer, *Chinese Physics B* **22**(2) (2013), 024702, DOI: 10.1088/1674-1056/22/2/024702.
- [5] K. Bhattacharyya, Effects of heat source/sink on MHD flow and heat transfer over a shrinking sheet with mass suction, *Chemical Engineering Research Bulletin* **15**(1) (2011), 12 – 17, DOI: 10.3329/ceerb.v15i1.6524.
- [6] L. Crane, Flow past a stretching plate, *Zeitschrift für angewandte Mathematik und Physik ZAMP* **21** (1970), 645 – 647, DOI: 10.1007/BF01587695.
- [7] T. Fang and J. Zhang, Closed-form exact solutions of MHD viscous flow over a shrinking sheet, *Communications in Nonlinear Science and Numerical Simulation* **14**(7) (2009), 2853 – 2857, DOI: 10.1016/j.cnsns.2008.10.005.
- [8] T. Fang and J. Zhang, Thermal boundary layers over a shrinking sheet: an analytical solution, *Acta Mechanica* **209** (2010), 325 – 343, DOI: 10.1007/s00707-009-0183-2.
- [9] T. Fang, J. Zhang and S. Yao, Viscous flow over an unsteady shrinking sheet with mass transfer, *Chinese Physics Letters* **26**(1) (2009), 014703, DOI: 10.1088/0256-307X/26/1/014703.
- [10] T. Hayat, Z. Abbas and M. Sajid, On the analytic solution of magnetohydrodynamic flow of a second grade fluid over a shrinking sheet, *Journal of Applied Mechanics* **74**(6) (2007), 1165 – 1171, DOI: 10.1115/1.2723820.

- [11] W. Ibrahim and O. D. Makinde, Magnetohydrodynamic stagnation point flow and heat transfer of casson nanofluid past a stretching sheet with slip and convective boundary condition, *Journal of Aerospace Engineering* **29**(2) (2016), 04015037, DOI: 10.1061/(ASCE)AS.1943-5525.0000529.
- [12] A. K. Jhankal and M. Kumar, MHD boundary layer flow past a stretching plate with heat transfer, *International Journal of Engineering Science* **2**(3) (2013), 9 – 13.
- [13] A. K. Jhankal and M. Kumar, MHD boundary layer flow past over a shrinking sheet with heat transfer and mass suction, *International Journal of Computational and Applied Mathematics* **12**(2) (2017), 441 – 448.
- [14] W. A. Khan, O. D. Makinde and Z. H. Khan, Non-aligned MHD stagnation point flow of variable viscosity nanofluids past a stretching sheet with radiative heat, *International Journal of Heat and Mass Transfer* **96** (2016), 525 – 534, DOI: 10.1016/j.ijheatmasstransfer.2016.01.052.
- [15] T. K. Kravchenko and A. I. Yablonskii, A boundary value problem on a semi-infinite interval, *Differential'nye Uraneniya* **8**(2) (1972), 2180 – 2186.
- [16] T. K. Kravchenko and A. I. Yablonskii, Solution of an infinite boundary value problem for third order equation, *Differential'nye Uraneniya* **1** (1965), 327.
- [17] R. B. Kudenatti, V. B. Awati and N. M. Bujurke, Approximate analytical solutions of a class of boundary layer equations over nonlinear stretching surface, *Applied Mathematics and Computation* **218**(6) (2011), 2952 – 2959, DOI: 10.1016/j.amc.2011.08.049.
- [18] S. Liao, A new branch of solutions of boundary-layer flows over an impermeable stretched plate, *International Journal of Heat and Mass Transfer* **49**(12) (2005), 2529 – 2539, DOI: 10.1016/j.ijheatmasstransfer.2005.01.005.
- [19] E. Magyari and B. Keller, Heat and mass transfer in the boundary layers on an exponentially stretching continuous surface, *Journal of Physics D: Applied Physics* **32**(5) (1999), 577 – 585, DOI: 10.1088/0022-3727/32/5/012.
- [20] O. D. Makinde, Analysis of Sakiadis flow of nanofluids with viscous dissipation and Newtonian heating, *Applied Mathematics and Mechanics* **33** (2012), 1545 – 1554, DOI: 10.1007/s10483-012-1642-8.
- [21] O. D. Makinde and A. Aziz, Boundary layer flow of a nanofluid past a stretching sheet with a convective boundary condition, *International Journal of Thermal Sciences* **50**(7) (2011), 1326 – 1332, DOI: 10.1016/j.ijthermalsci.2011.02.019.
- [22] O. D. Makinde, Computational modelling of nanofluids flow over a convectively heated unsteady stretching sheet, *Current Nanoscience* **9**(5) (2013), 673 – 678, DOI: 10.2174/15734137113099990068.
- [23] O. D. Makinde, F. Mabood, W. A. Khan and M. S. Tshelha, MHD flow of a variable viscosity nanofluid over a radially stretching convective surface with radiative heat, *Journal of Molecular Liquids* **219** (2016), 624 – 630, DOI: 10.1016/j.molliq.2016.03.078.
- [24] O. D. Makinde, V. B. Awati and N. M. Bujurke, Dirichlet series and closed-form exact solutions of MHD casson fluid flow over a permeable stretching/shrinking sheet, *Palestine Journal of Mathematics* **10**(1) (2021), 109 – 119, URL: https://pjm.ppu.edu/sites/default/files/papers/PJM_NOV_2020_109_to_119.pdf.
- [25] M. Miklavčič and C. Y. Wang, Viscous flow due to a shrinking sheet, *Quarterly of Applied Mathematics* **64** (2006), 283 – 290, DOI: 10.1090/S0033-569X-06-01002-5.
- [26] M. Mustafa, T. Hayat, P. Ioan and A. Hendi, Stagnation-point flow and heat transfer of a casson fluid towards a stretching sheet, *Zeitschrift für Naturforschung A* **67**(1-2) (2012), 70 – 76, DOI: 10.5560/zna.2011-0057.

- [27] S. Nadeem and M. Awais, Thin film flow of an unsteady shrinking sheet through porous medium with variable viscosity, *Physics Letters A* **372**(30) (2008), 4965 – 4972, DOI: 10.1016/j.physleta.2008.05.048.
- [28] S. Nadeem, R. U. Haq and C. Lee, MHD flow of a Casson fluid over an exponentially shrinking sheet, *Scientia Iranica* **19**(6) (2012), 1550 – 1553, DOI: 10.1016/j.scient.2012.10.021.
- [29] N. F. M. Noor, O. Abdulaziz and I. Hashim, MHD flow and heat transfer in a thin liquid film on an unsteady stretching sheet by the homotopy analysis method, *International Journal for Numerical Methods in Fluids* **63**(3) (2010), 357 – 373, DOI: 10.1002/flid.2078.
- [30] N. F. M. Noor, S. A. Kechil and I. Hashim, Simple non-perturbative solution for MHD viscous flow due to a shrinking sheet, *Communications in Nonlinear Science and Numerical Simulation* **15**(2) (2010), 144 – 148, DOI: 10.1016/j.cnsns.2009.03.034.
- [31] B. C. Sakiadis, Boundary-layer behavior on continuous solid surfaces: II. The boundary layer on a continuous flat surface, *AIChE Journal* **7**(2) (1961), 221 – 225, DOI: 10.1002/aic.690070211.
- [32] F. K. Tsou, E. M. Sparrow and R. J. Goldstain, Flow and heat transfer in the boundary layer on a continuous moving surface, *International Journal of Heat and Mass Transfer* **10**(2) (1967), 219 – 235, DOI: 10.1016/0017-9310(67)90100-7.
- [33] C. Y. Wang, Exact solutions of the steady-state Navier-Stokes equations, *Annual Review of Fluid Mechanics* **23**(1) (1991), 159 – 177, DOI: 10.1146/annurev.fl.23.010191.001111.
- [34] C. Y. Wang, Stagnation flow towards a shrinking sheet, *International Journal of Non-Linear Mechanics* **43**(5) (2008), 377 – 382, DOI: 10.1016/j.ijnonlinmec.2007.12.021.

